Masters Report
University of Toronto Department of Physics

August 2009

Dark Matter, Supersymmetry and the ATLAS Detector

Sheetal Saxena

Contents

1 Introduction

The term 'Dark Matter' is fitting in both the physical description of the phenomena as well as of its understanding. It has never been directly observed or manipulated by scientists but rather acknowledged as a reasonable explanation for indirect observations made throughout history. It is the favored theory however, as it requires the fewest deviations from known science. The first observation of an anomaly in the skies was in 1933 by astrophysicist Fritz Zwicky (1). He attempted to calculate the mass of the Coma Cluster of Galaxies, which contains over 1000 galaxies. The method was simple, to derive the total mass from the orbital velocities of galaxies on the cluster's edges. However this yielded an expected mass much greater than accounted for by the number of galaxies in the cluster. Zwicky concluded that a non-visible and elusive form of matter was holding the cluster together through its gravitational effects; and hence coined the term 'Dark Matter.'

Today, scientists agree that the stars, suns and dust that constitute known and recorded forms of matter total to only 5% of the matter in the universe. The 95% that is unaccounted for prevents galaxies from flying apart, controls galactic rotation curves, and bends light to produce gravitational lensing effects [1].

2 Evidence

2.1 On the galactic scale

2.1.1 Galaxy Rotation Curves

The most direct and convincing evidence for dark matter on the galactic scale comes from plotting the circular velocities of stars as a function of their distance from the galactic centre. American astrophysicist Vera Rubin is credited for pioneering work on “The Galaxy Rotation Problem,” after Zwicky's initial observation. She closely analyzed the discrepancy between the observed angular momentum of galaxies and their predicted values. The observed motion is that speed is directly proportional to radius, implying a 'flat' distribution of mass and gravitational force through the spiral. See a typical example in Figure 1, where 'disk' represents the Keplerian predicted velocity distribution. The uppermost curve with error bars is the observed velocity distribution. This implies a relatively even distribution of matter throughout the spiral beyond the central bulge.

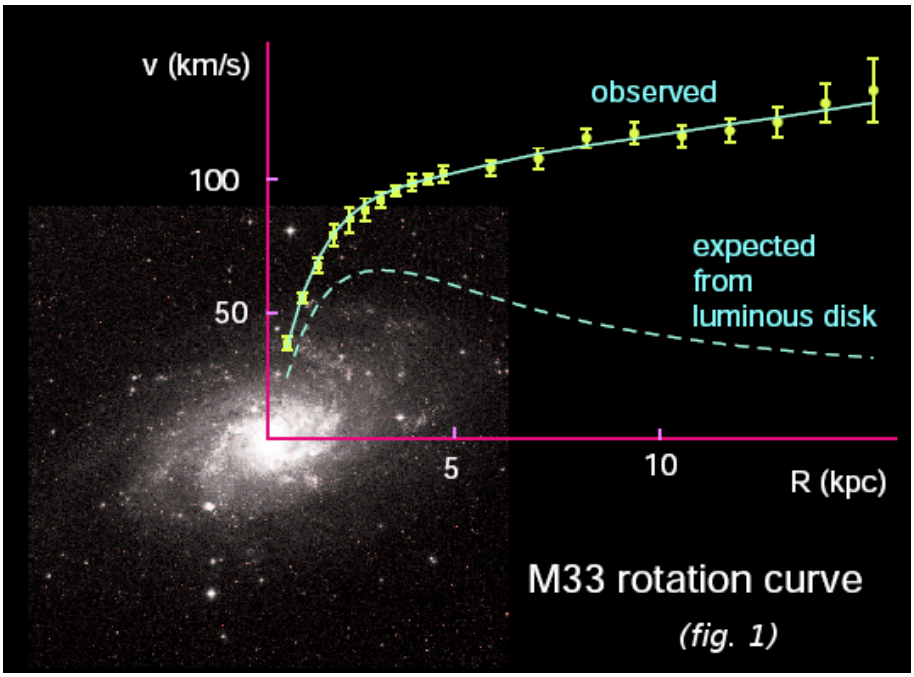

Figure 1: The rotation curve for the Spiral Galaxy M33. Points represent the measured rotation velocities and the dashed curve is expected due to the observed dark matter. The existence of dark matter is inferred by the discrepancy between the observed rotation curve and the one due to the luminous disk [13].

For a galaxy of mass m to orbit in a cluster, its centripetal force must match the gravitational force from the central bulge M:

$$\frac{GMm}{r^2} = \frac{mv^2}{r} \tag{1}$$

So that the expected velocity is

$$v = \sqrt{\frac{GM}{r}} \tag{2}$$

This is the expected disk curve shown in Figure 2, dropping off after the central bulge as 1/√r.

In reality, the curve looks like the uppermost curve, with velocity remaining constant with r. Adding another mass term m(r) to represent dark matter as a function of radius:

$$\frac{G\left[M+m(r)\right]}{r^2}=\frac{v^2}{r} \tag{3}$$

$$v=\sqrt{\frac{GM}{r}+\frac{Gm(r)}{r}} \tag{4}$$

Taking r going to infinity:

$$v=\sqrt{\frac{Gm(r)}{r}} \tag{5}$$

The curve can be explained if m(r) is directly proportional to r:

$$m(r)\propto r \tag{6}$$

So that velocity remains constant:

$$v=\sqrt{Gm_0} \tag{7}$$

where as usual

$$m(r)=4\pi\int_0^r \rho(r')r'^2dr' \tag{8}$$

and

$$\rho(r')$$

is the mass density profile, and should be falling off as $1/\sqrt{r}$ beyond the disk. The fact that v(r) is constant implies the existence of a halo with m(r) α r and r_o α $1/r^2$. At some point r_o will have to fall off faster, in order to keep the total mass of the galaxy finite. This exact radius is as of yet unknown, leading to a lower bound on the dark matter mass density: $\Omega_{DM} > 0.1$, where $\Omega_X \equiv r_{oX}/r_{ocrit}$, and r_{ocrit} is the critical mass density. Note: $\Omega_{tot} = 1$ corresponds to a flat universe [8].

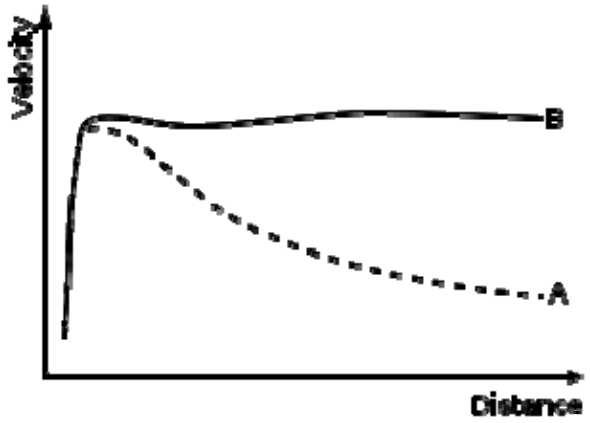

Figure 2: Idealized plot of galaxy velocity with respect to radius. Curve A represents the Keplerian predicted velocity distribution. Curve B is the observed velocity distribution [6].

2.1.2 Gravitational lensing

Following from Einstein's theory of general relativity, light propagates along geodesics which deviate from straight lines when passing near intense gravitational fields. The shape of the potential well and thus the mass of a cluster can be inferred by the distortion of the images of the background objects due to the gravitational mass of the cluster. Note the clear gravitation arcs in the Hubble images of Figure 3.

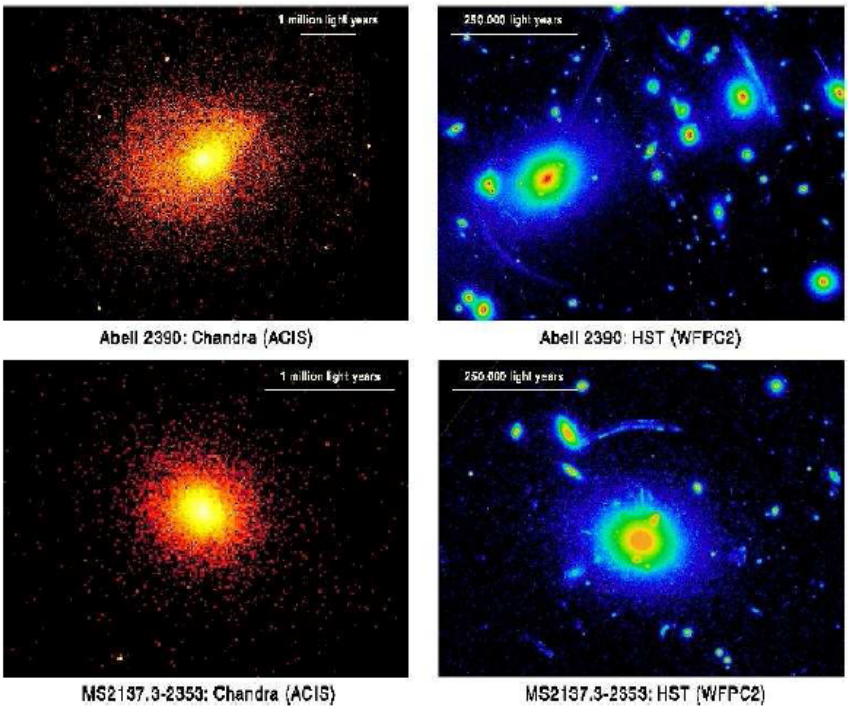

Figure 3: Chandra X-ray and Hubble Space Telescope Images (left, right) of Abell 2390 and MS2137.3-2353 [4].

The effects of gravitational lensing can thus be used to map dark matter. The curving of light rays around large masses is a particularly useful probe for studying dark matter because it is independent of the nature of the mass. A favorite is the 'Bullet Cluster' example, which Nasa deemed 'Direct Proof of Dark Matter' in 2006. The Chandra X-Ray Observatory observed the hundred-million degree hot gas shaped into a bullet due to wind produced by the collision of two clusters. The hot gas was slowed by drag forces analogous to air resistance, while the dark matter components of both clusters passed directly through one another as they do not interact in any way except for gravitational effects. As a result the dark matter and normal matter were separated. The dark matter location was accurately determined as it distorted light rays emitted from known galaxies in the background. This is shown as regions A and D in Figure 4. Regions B and C are hot gases which collided and passed through each other but were slowed via electromagnetic drag forces, observed by X-ray emission data. The majority of the mass is in the blue areas, implying the existence of dark matter. Results were subsequently confirmed by the Hubble Space Telescope, Magellan optical telescopes and the European Southern Observatory [5]. The mass density contours as determined by The Hubble Space Telescope are shown in Figure 5. Observations of clusters of galaxies such as this tend to give somewhat larger values; Ω_{DM} = 0.2 to 0.3 [8].

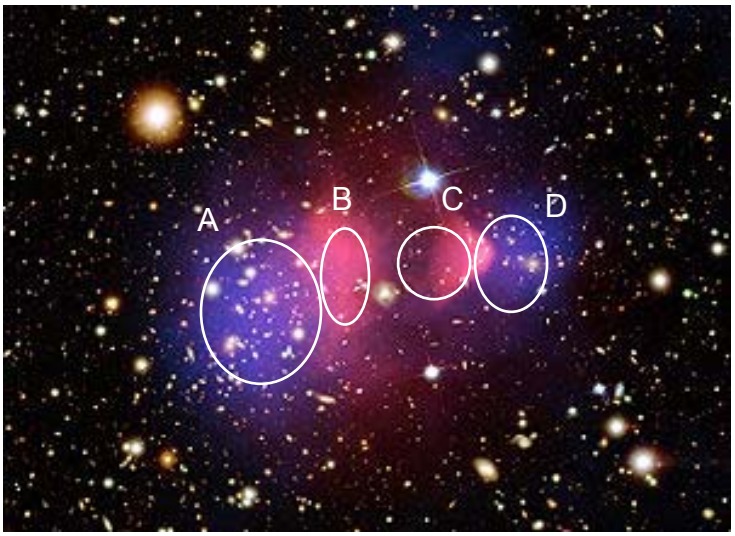

Figure 4: Image of both clusters post-collision. The majority of the mass is not located where X-ray emission data expects, implying the existence of dark matter [5].

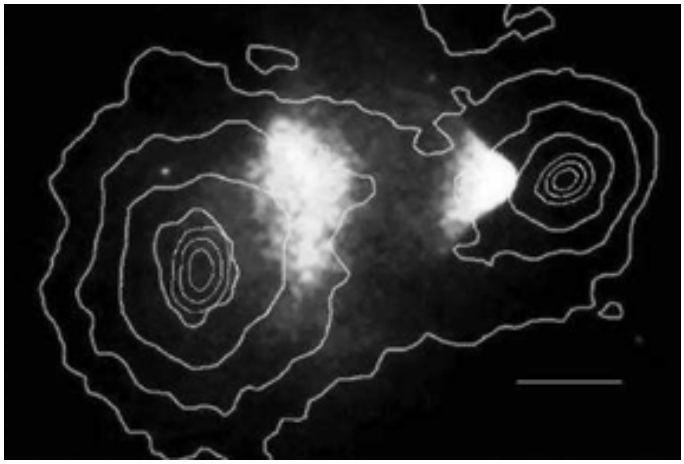

Figure 5: Surface mass density contours from lensing effects [6].

2.2 On the cosmological scale

2.2.1 Cosmic microwave background and evidence from WMAP

Another key line of evidence for dark matter is the anisotropy of the Cosmic Microwave background (CMB) which has been probed experimentally in great detail. Advances in observational cosmology are leading to the establishment of the fist precision cosmological model, with key cosmological parameters determined to one or two significant figure accuracy. The currently most accurate determination of Ω_{DM} comes from these global fits of cosmological parameters based on measurements from WMAP [8]. The Wilkinson Microwave Anisotropy Probe (WMAP) is a satellite built to measure the temperature of the remnant radiant heat from the Big Bang. Launched in 2001, its objective was to create a full-sky map of the CMB by observing light emanating from the universe billions of years ago (See Figures 6). Data has been released at the one, three and five year points since launching. The originally proposed duration of 8 observing years will end in September 2009 [7].

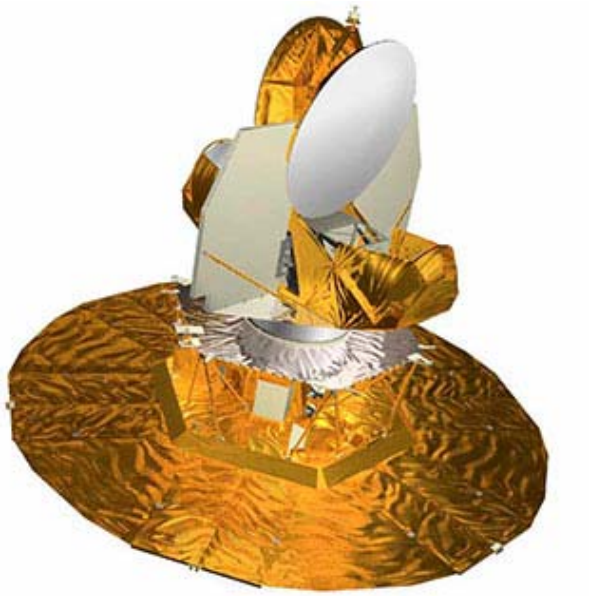

Figure 6: The Wilkinson Microwave Anisotropy Probe [11].

Recent data from WMAP has confirmed with great accuracy that the age of the Universe is 13.7 Billion years old, and the current energy density of the Universe is comprised of 72% dark energy, and 23% non-baryonic dark matter. The remaining 5% is baryonic matter. See Figure 7. The density of cold, non-baryonic matter is taken to be

$\Omega_{nbm}h^2 = 0.106 \pm 0.008$ (9)

where h is the Hubble constant in units of 100km/(s·Mpc). The baryonic matter density is taken to be

$\Omega_b h^2 = 0.022 \pm 0.001$ [8]. (10)

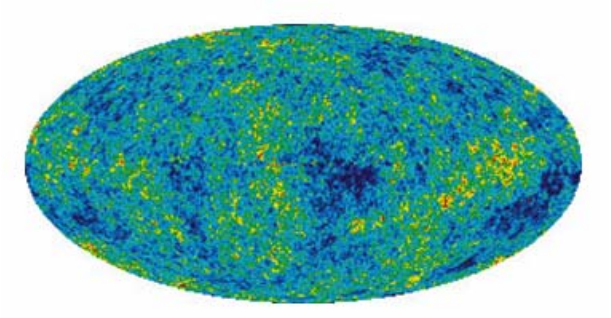

Figure 7: 5-year data revealed the average temperature of the universe as 2.725K or -270 degrees Celsius. CMB temperature fluctuations are shown by color differences; red representing warm regions and blue, cold regions [7].

Nojiri, Polesello and Tovey studied the consistency of the signal with astrophysical and non-accelerator constraints on SUSY Dark Matter in 2005 [16], based on measurements of end-points and thresholds in the invariant mass spectra of various combinations of jets and leptons. The measurements were used to constrain the SUSY breaking parameters in the MSSM model. Based on these constraints, the accuracy with which the Dark Matter relic density can be measured was assessed [16]. Figure 8 shows the predicted relic density as a function of LSP mass, produced by Monte Carlo simulation for a tau tau cross section of 1 GeV ($\sigma(m(\tau\tau)) = 1$ GeV). A line at $\Omega_{nbm}h^2 = 0.106 \pm 0.008$ has been superimposed to illustrate the range of LSP mass for the WMAP predicted relic density value.

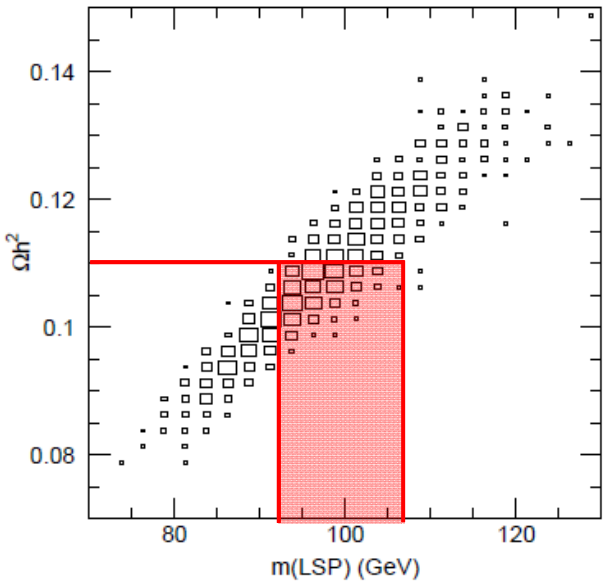

Figure 8: Value of the predicted relic density as a function of the measured LSP mass [16].

3 The Matter Density of the Universe

Following from The Concordance Model of Cosmology, The 'Critical Density' Ω_c is the average density of matter in the universe today that would be needed to, at some point in the future, exactly halt cosmic expansion. The distortion of spacetime due to gravitational effects of matter can only have three possible forms: a universe with precisely the critical density is Euclidean or Flat. A universe with density greater than Ω_c will eventually stop expanding, contract and implode under its own gravitational pull (closed universe scenario) and an open universe with density less than Ω_c will cause cosmic expansion that continues forever. See Figure 9.

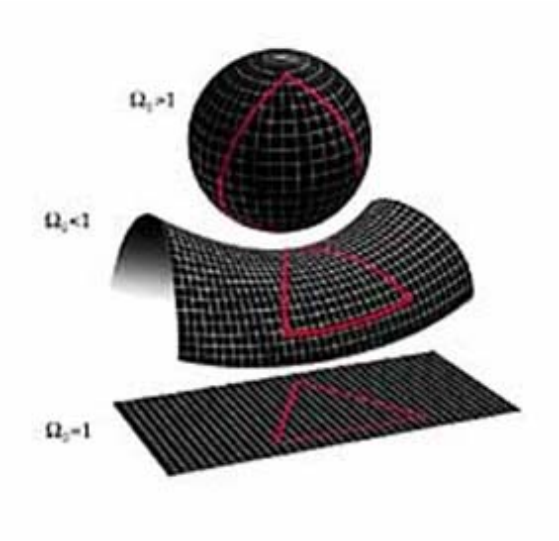

Figure 9: The possible spacetime geometries [12].

WMAP has confirmed the curvature of spacetime to within 1% of Flat-Euclidean, improving on the precision of previous measurements by over an order of magnitude.

The total density parameter of the universe consists of three major contributors, where $\Omega_o = 1$ for a critical density universe.

$$\Omega_o = \Omega_m + \Omega_{rel} + \Omega_\Lambda \quad (11)$$

Ω_m is the mass density, including ordinary and dark matter.
Ω_{rel} is the effective mass density of relativistic particles, photons and neutrinos.
Ω_Λ is the effective mass density of dark energy, described as the cosmological constant. The best estimates from WMAP are as follows, where only a small fraction of
Ω_m is ordinary matter, it mostly constitutes dark matter.

$$\Omega_m = 0.27 \pm 0.016 \quad (12)$$

$$\Omega_{rel} = 5.934 \pm 0.008x10\text{-}5 \quad (13)$$

$$\Omega_\Lambda = 0.72 \pm 0.08 \quad (14)$$

4 Candidate Particles

4.1 Requirements for candidate particles

The first requirement on the candidate particles for dark matter is that they must account for the 23% of the Universe's mass density that is designated as dark matter. Analysis of structure formation in the universe has indicated that dark matter should have been non-relativistic at the onset of galaxy formation, ie: when there was a galactic mass inside the causal horizon. It must be non-relativistic or “cold” meaning that the candidate particles do not travel at speeds approaching the speed of light and thus tend to clump together under their own gravity. This is in agreement with the upper bound on the contribution to non- (15) baryonic matter density (Equation 9) from light neutrinos:

$\Omega_v h^2 \leq 0.0076$ 95% CL.

Additional requirements for non-baryonic dark matter candidates are that they must interact very weakly with electromagnetic radiation and be stable on cosmological time scales otherwise would have decayed by now.

4.2 The Axion

The elegant solution put forth by Peccei and Quinn for the “strong CP problem” was of a new global symmetry (U(1)) that is spontaneously broken at large energy scales, allowing the restoration of CP symmetry in Quantum Chromodynamics (the theory of the strong interaction). The consequence resulting from this mechanism is the axion, which is a new pseudoscalar boson [10]. Axions are very light, and remain a dark matter candidate.

4.3 The Neutralino

Thermally produced Weakly interacting massive particles (WIMPS) X are particles of mass 10 GeV to 1 TeV with cross sections on the weak interaction scale. Neutralinos in models of R-parity conserving supersymmetry are by far the most widely studied dark matter candidate. The neutralino is considered the lightest supersymmetric particle, which is stable thus has no further decay modes. R-parity is a symmetry acting on the Minimal Supersymmetric Standard Model (mSUGRA), with equation:

$R = (-1)^{2j+3B+L}$

Where j is the spin, B is the baryon number and L is the lepton number. All supersymmetric particles have an R-parity of -1, while standard model particles have R-parity of +1. R-parity is a multiplicative symmetry meaning that the initial state has a total R-parity of +1 so every following vertex will have two supersymmetric particles and one standard model particle to conserve the

symmetry. What eventually results from the cascade are high transverse momentum (p_T) quarks, leptons, and the lightest supersymmetric particle.

The most widely studied WIMP is the lightest neutralino. Detailed calculations have shown that it has the required thermal relic density (Equation 9) in four regions of parameter space [8].

5 Scientific Motivation and Assumptions

5.1 Motivation for the Large Hadron Collider

There are several reasons that lend support to the expectation of finding supersymmetry at the Large Hadron Collider. The 14 TeV proton-proton synchrotron has been constructed for the purpose of testing various predictions made in theoretical high energy physics, including the remaining standard model particle, the Higgs Boson. It will be essential in the search for new particles predicted by supersymmetry, including dark matter candidates. The motivation for believing in supersymmetry includes idealistic points such as its intrinsic elegance, ability to link gravity to other fundamental interactions, and link matter particles and force carriers. There are substantial reasons to expect supersymmetry will appear at an energy accessible to the LHC. First is the observation that supersymmetry can stabilize the mass scale of electroweak symmetry breaking. This suggests that supersymmetric particles have masses less than 1 TeV. Secondly, it has been observed that the LSP in such aforementioned R-parity conserving models will be an excellent dark matter candidate. This motivation requires that the LSP weighs less than 1 TeV [14].

5.2 Unification of Forces

The third reason for expecting to see supersymmetry at the LHC is the observation that the inclusion of supersymmetric particles in the renormalization group equations for the gauge couplings of the Standard Model will allow them to unify [14]. A key working assumption has been taken that the electromagnetic force, weak force and strong force are unified when supersymmetry is considered. Figure 10 shows that energies up to 100 GeV have already been probed by The Large Electron Positron Collider (LEP) at CERN, and that a direct extrapolation would not have the forces unify. Including supersymmetry and extrapolating using the renormalization group equations, mainly from pivotal work done by Frank Wilczek et. al, shows the forces unify at the 10^{16} GeV scale.

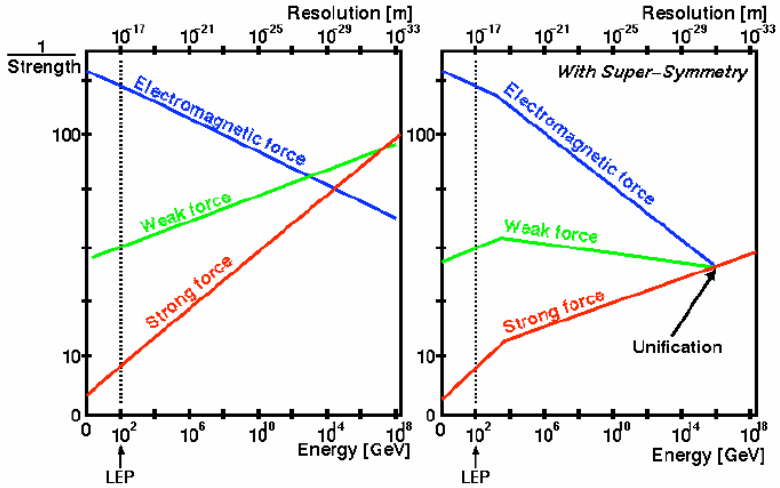

Figure 10: The unification of forces with supersymmetry [13].

In the Minimal Supersymmetric Standard Model, quark masses and supersymmetric gluino masses unify at higher energies. See Figure 11.

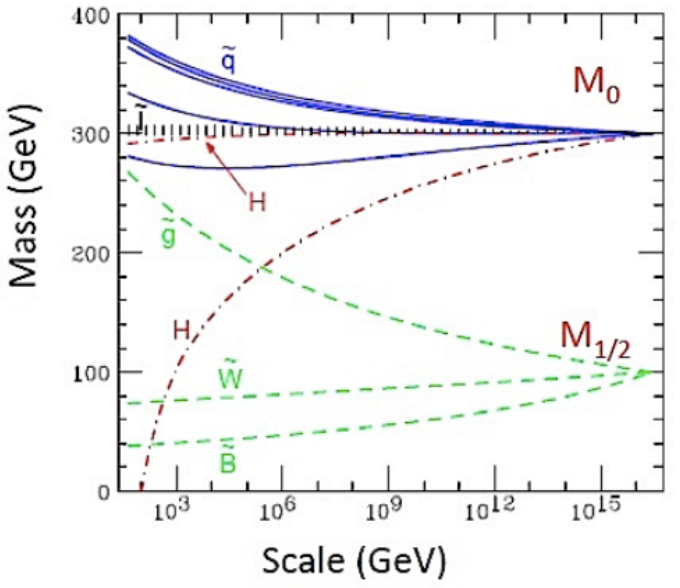

Figure 11: Spin 0 sfermions unify to M_0 and spin ½ gauginos unify to $M_{1/2}$ at the unification scale [13].

6 Constraints from Experiment

6.1 Large Electron Positron Collider

The LEP collider began operation in August 1989, accelerating electrons and positrons up to 45 GeV each to produce the Z boson of mass 91 GeV. A later upgrade also made the production of two W bosons possible, each of 80 GeV. It was dismantled in 2000 for the construction of the Large Hadron Collider in the same tunnel. LEP was a pivotal experiment in high energy physics because it allowed confirmation of several Standard Model quantities through its precision measurements. Measurements of the shape of the Z boson mass peak revealed the constraint that the number of light neutrinos is limited to three.

6.2 Tevatron

The Tevatron is a circular 2 TeV proton-antiproton synchrotron located at Fermilab. It was completed in 1983 and has undergone regular upgrades since then, but will cease operation in 2010 as it is obsolete by the LHC. It made possible the discovery of the top quark in 1995 and then the measurement of its mass to a precision of within 1% in 2007.

6.3 Overview of Constraints

M_0 $M_{1/2}$ planes have become a very useful way to communicate information about constraints from previous experiments such as LEP, the Tevatron and Cosmology, and the preferred regions for finding Susy. The parameters are defined in the Constrained minimal extension to the standard model (CMSSM) as follows:

M_0 is the scalar mass parameter
$M_{1/2}$ is the gaugino mass parameter
Tanβ is the ratio of the Higgs vacuum expectation value
μ is the sign of the supersymmetric Higgs parameter
A_0 is the trilinear coupling

Assuming that the LSP is the lightest neutralino X and enforcing the relic density constraint (Equation 9) limits one to narrow WMAP strips in projections of the MSSM parameters. The X densiry would be dependent on the expansion rate at the freeze-out temperature which is approximately 1/25 of m_X [15] and in the GeV range. As well, SUSY might not be the only contributor to the cold dark matter, and most simple SUSY models present a relic density that is greater than the WMAP range (Equation 9). The WMAP strips are significantly varied depending on the choices of Tanβ. The plots below are in the CMSSM where SUSY breaking scalar masses M_0 and gaugino masses $M_{1/2}$ are each assumed to be universal at the Unification scale. As Tanβ is varied, the WMAP strips cover much of the plane. Figure 12 shows the M_0 $M_{1/2}$ plane in the CMSSM for a Higgs

vacuum expectation ratio of 10, and a positive Higgs parameter. The nearly vertical red line is the contour for a Higgs mass of 114 GeV and the nearly vertical black line is the contour for the mass of a Chargino, 104 GeV. Several different regions of the CMSSM plane can be distinguished, in which different dynamical processes are dominant. Data from LEP experiments have been compiled and are represented by the blue curve in the lower left corner, showing the bound for the mass of the supersymmetric electron. Thus its mass must be greater than 99 GeV. The dark green region is excluded by b → s + gamma, in the minimal flavor violating case. The brown region is excluded because there is no neutral LSP (there is only the charged LSP, the supersymmetric tau). The pink area shows the region allowed from an electroweak correction, in the 1 sigma range and the 2 sigma range. The turquoise region is the cosmologically preferred region [14]. When the vacuum expectation value is instead 50 for a positive Higgs parameter, all regions become expanded and range to much higher values of M_0 and $M_{1/2}$. The brown region indicating no neutral LSP covers half the plane and the cosmologically preferred region is also shifted.

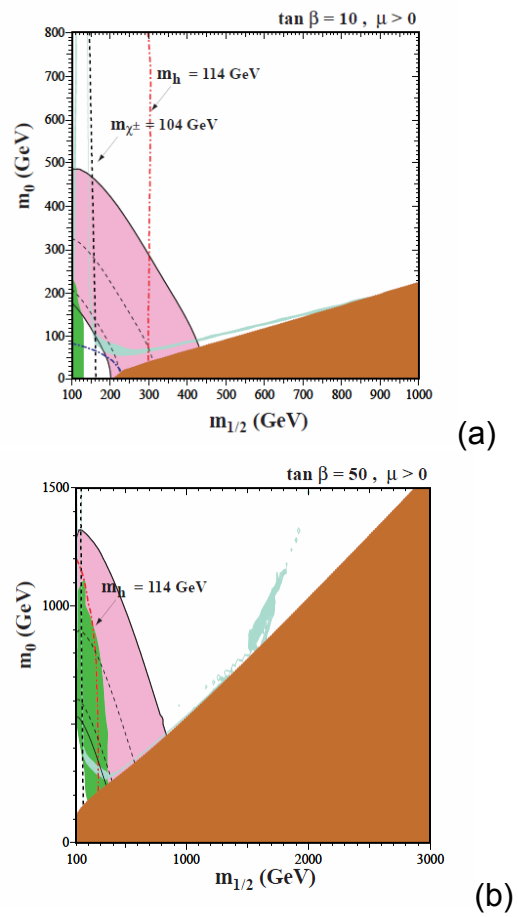

Figure 12: The CMSSM planes for (a) Tanβ = 10, μ > 0 and (b) Tanβ = 50, μ > 0 [14].

7 Searches at ATLAS

For Supersymmetry analysis at the ATLAS detector, a set of benchmark points in the minimal supergravity frameworks have been chosen, with the aim of exploring sensitivity to a wide class of final-state signatures. They are defined in terms of the minimal supergravity parameters at the unification scale, with A_0 the trilinear coupling, and X_1 the LSP neutralino for minimal supergravity. See Appendix A.

A particularly useful plot in the ATLAS group is shown below in Figure 13, which superimposes the chosen points of interest over the M_0 $M_{1/2}$ planes from [14]. SU3 and SU4 clearly fall into the turquoise cosmologically preferred region.

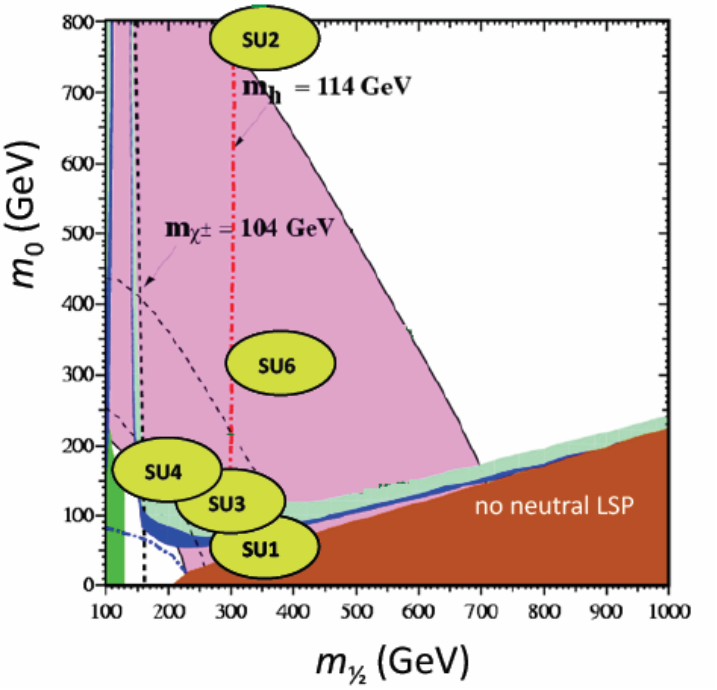

Figure 13: ATLAS points of interest in the M_0 $M_{1/2}$ plane [13].

The recent ATLAS-specific publication “Prospects for Supersymmetry and Universal Extra Dimensions discovery based on inclusive searches at a 10 TeV centre-of-mass energy with the ATLAS detector” estimates for 0-lepton channels and multi-lepton channels at 200 inverse picobarn integrated luminosity for a 10 TeV centre of mass energy. See Figure 14. Figure 15 shows the 5σ discovery reach for the mSUGRA model with tanb = 10 and tanb = 50 respectively for the 4 jet 0 lepton, the 4 jet 1 lepton and the 2 jet 2 lepton channels [15].

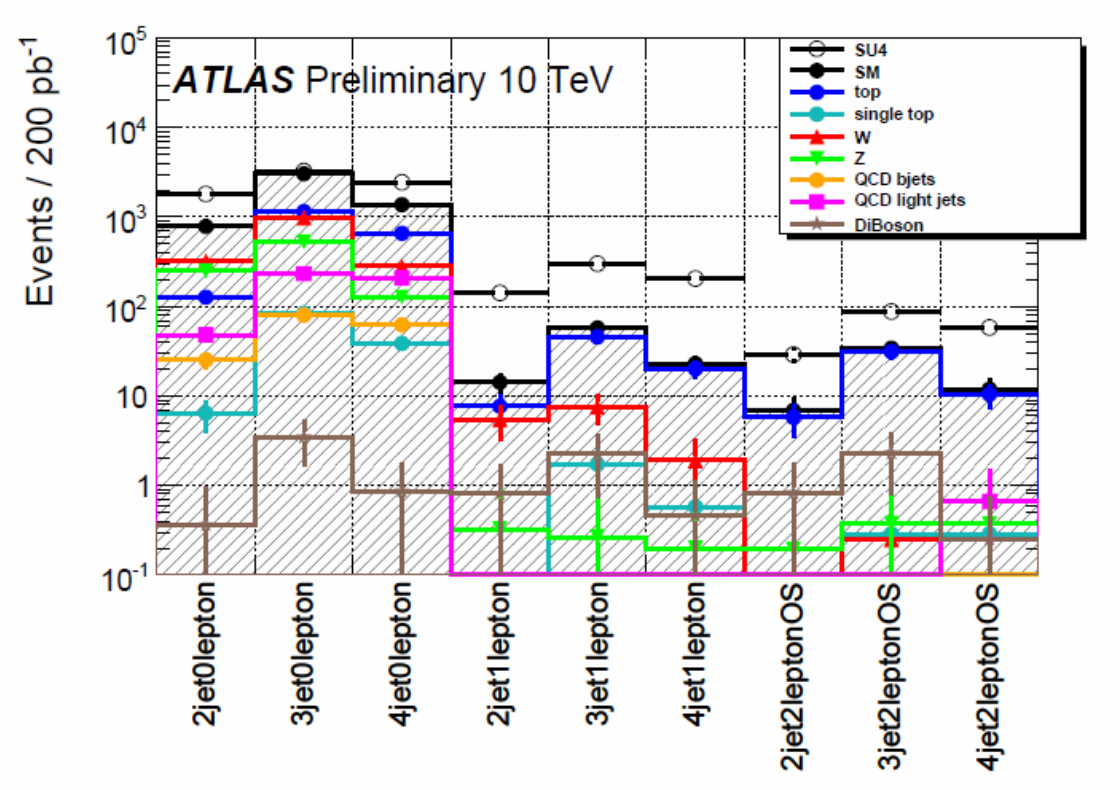

Figure 14: ATLAS 10 TeV Estimate [15].

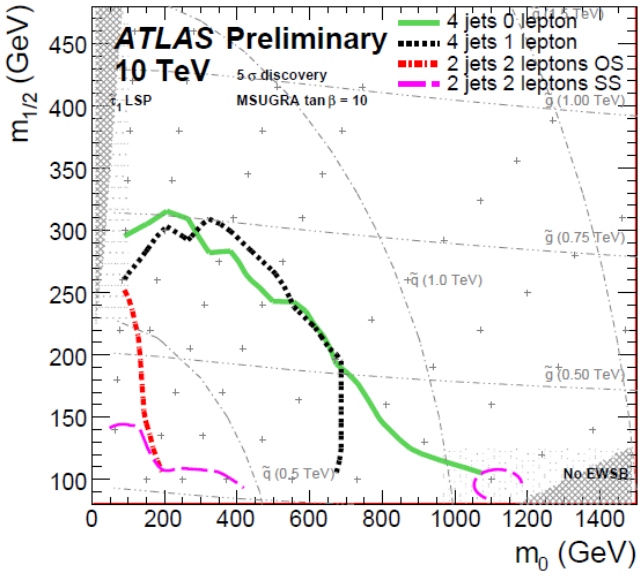

(a)

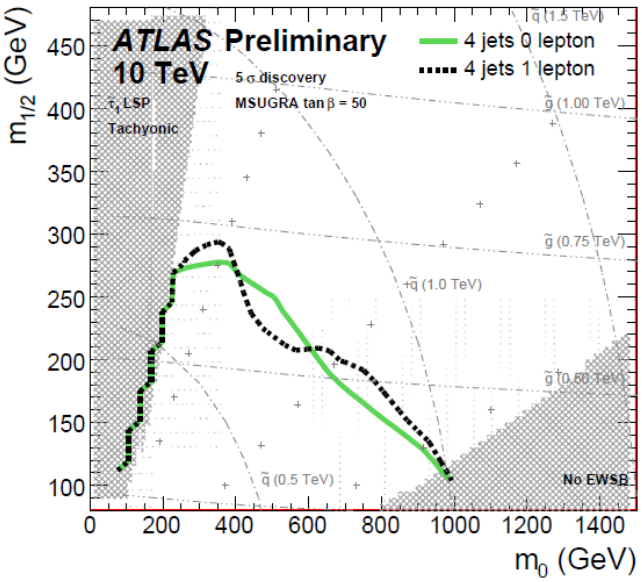

(b)

Figure 15: (a) 5σ discovery reach as a function of m0 and m1/2 for tanb = 10 mSUGRA scan for channels with 0, 1 and 2 leptons. Only the channels with the largest discovery reach are shown for each lepton multiplicity. (b) 5σ discovery reach as a function of m0 and m1/2 for tanb = 50 mSUGRA scan for channels with 0 and 1 leptons.

In [16], monte carlo experiments are used to produce distributions of the calculated relic densities as shown, using soft MSSM parameters as input, for two values of the assumed uncertainty on the position of the tau tau edge. Figure 16 shows the distributions of the predicted relic density incorporating the experimental errors. The distributions are shown for an assumed error on the tt edge respectively of 5 GeV (left) and 0.5 GeV (right).

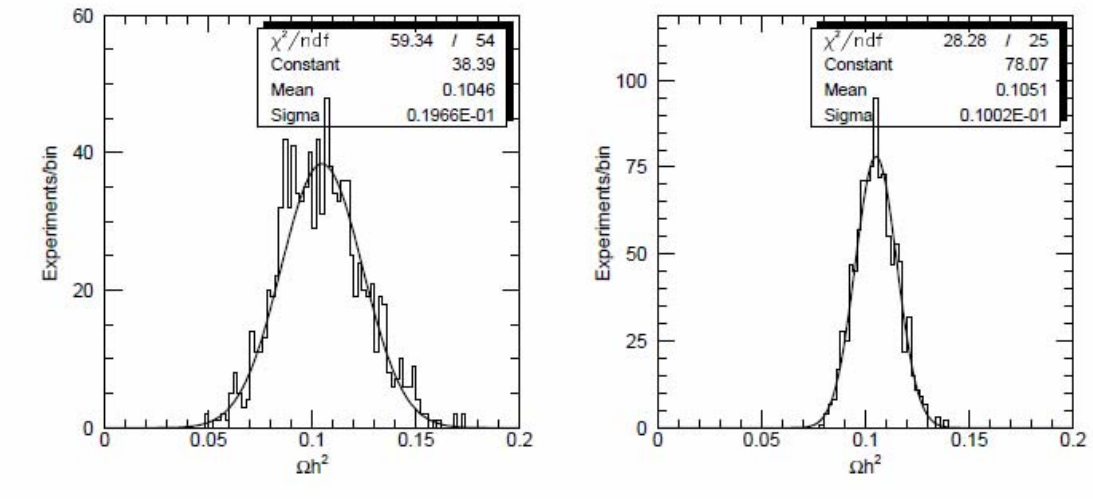

Figure 16: Distributions of the predicted relic density incorporating experimental error. (a) Assumed error on tt *edge of 5 GeV. (b) Assumed error on* tt *edge of 0.5 GeV.*

8 Conclusion

Evolution in the understanding of Dark Matter have seen exponential success since its initial discovery. Pioneered by Zwicky and Rubin's observations of the anomalies in the skies, major space stations and earth based telescopes have continued to explore the concept of dark matter. At present, numerical quantities describing the matter density, temperature fluctuations and age of the Universe are known with high precision. Combining these constraints with results from collider experiments have yielded highly detailed requirements on the possible candidate particles for dark matter, as well as expected regions for SUSY particles. It is anticipated that much high energy and astrophysical theory will be confirmed or debunked in the next 10 years as the Large Hadron Collider begins operation and as data analysis techniques at ATLAS evolve. It can be expected that science will soon have a deeper grasp of this subject which will contribute to the overall understanding of matter and the cosmos.

Appendix A

Susy points of interest at the ATLAS detector [13].

SU1 $m_0 = 70$ GeV, $m_{1/2} = 350$ GeV, $A_0 = 0$, $\tan\beta = 10$, $\mu > 0$. Coannihilation region where $\tilde{\chi}_1^0$ annihilate with near-degenerate $\tilde{\ell}$.

SU2 $m_0 = 3550$ GeV, $m_{1/2} = 300$ GeV, $A_0 = 0$, $\tan\beta = 10$, $\mu > 0$. Focus point region near the boundary where $\mu^2 < 0$. This is the only region in mSUGRA where the $\tilde{\chi}_1^0$ has a high higgsino component, thereby enhancing the annihilation cross-section for processes such as $\tilde{\chi}_1^0\tilde{\chi}_1^0 \to WW$.

SU3 $m_0 = 100$ GeV, $m_{1/2} = 300$ GeV, $A_0 = -300$ GeV, $\tan\beta = 6$, $\mu > 0$. Bulk region: LSP annihilation happens through the exchange of light sleptons.

SU4 $m_0 = 200$ GeV, $m_{1/2} = 160$ GeV, $A_0 = -400$ GeV, $\tan\beta = 10$, $\mu > 0$. Low mass point close to Tevatron bound.

SU6 $m_0 = 320$ GeV, $m_{1/2} = 375$ GeV, $A_0 = 0$, $\tan\beta = 50$, $\mu > 0$. The funnel region where $2m_{\tilde{\chi}_1^0} \approx m_A$. Since $\tan\beta \gg 1$, the width of the pseudoscalar Higgs boson A is large and τ decays dominate.

SU8.1 $m_0 = 210$ GeV, $m_{1/2} = 360$ GeV, $A_0 = 0$, $\tan\beta = 40$, $\mu > 0$. Variant of coannihilation region with $\tan\beta \gg 1$, so that only $m_{\tilde{\tau}_1} - m_{\tilde{\chi}_1^0}$ is small.

SU9 $m_0 = 300$ GeV, $m_{1/2} = 425$ GeV, $A_0 = 20$, $\tan\beta = 20$, $\mu > 0$. Point in the bulk region with enhanced Higgs production

References

[1] M. J. Rees, “Dark Matter Introduction.” February 2, 2004.
[2] V. Rubin, W. K. Ford. “Rotation of the Andromeda Nebula from a Spectroscopic Survey of Emission Regions”. Astrophysical Journal 159: 379.
[3] K. G. Begeman, A. H. Broeils and R. H. Sanders, 1991, MNRAS, 249, 523
[4] A. C. Fabian and S. W. Allen, Proceedings of the 21st Texas Symposium on Relativistic Astrophysics (Texas in Tuscany), Florence, Italy, 2002.
[5] Harvard Press Release, 2006. http://chandra.harvard.edu
[6] A. Heavens, “Weak Gravitational Lensing.” May 13, 2008.
[7] NASA Press Release, “NASA Finds Direct Proof of Dark Matter.” August 21, 2006. http://www.nasa.gov/home/hqnews.html
[8] PDG http://pdg.lbl.gov 22: Dark Matter
[9] J. Ellis, “Supersymmetric Dark Matter in Light of WMAP.” March 2003, CERN-TH/2003-051
[10] G. G. Raffelt, “Axions-Motivations, limits and searches.” November 2006.
[11] WMAP: Wilkinson Microwave Anisotropy Probe. Nasa. http://map.gsfc.nasa.gov/media/990293/index.html
[12] “Foundations of Big Bang Cosmology.” NASA, 2009. http://map.gsfc.nasa.gov/universe/bb_concepts.html
[13] Travis Bain. University of Toronto Phd Candidate.
[14] J. Ellis, “Prospects for Discovering Supersymmetry at the LHC.” October 7, 2008.
[15] “Prospects for Supersymmetry and Universal Extra Dimensions discovery based on inclusive searches at a 10 TeV centre-of-mass energy with the ATLAS detector.” ATLAS Note. http://cdsweb.cern.ch/record/1191916?ln=en
[16] Nojiri, Polesello and Tovey. “Constraining Dark Matter in the MSSM at the LHC.” December 2005, hep-ph/0512204v1